ISSN 0965-545X, Polymer Science, Series A, 2019, Vol. 61, No. 2, pp. 175–185. © Pleiades Publishing, Ltd., 2019.
Russian Text © A.E. Chalykh, U.V. Nikulova, A.A. Shcherbina, E.V. Chernikova, 2019, published in Vysokomolekulyarnye Soedineniya, Seriya A, 2019, Vol. 61, No. 2, pp. 152–162.

POLYMER BLENDS

Diffusion and Thermodynamics of Mixing of Polystyrene with Statistical Copolymers of Butyl Acrylate and Styrene

A. E. Chalykh[a], U. V. Nikulova[a,*], A. A. Shcherbina[a,b], and E. V. Chernikova[c,d]

[a] *Frumkin Institute of Physical Chemistry and Electrochemistry, Russian Academy of Sciences, Moscow, 119071 Russia*
[b] *Dmitry Mendeleev University of Chemical Technology of Russia, Moscow, 125047 Russia*
[c] *Faculty of Chemistry, Moscow State University, Moscow, 119991 Russia*
[d] *Topchiev Institute of Petrochemical Synthesis, Russian Academy of Sciences, Moscow, 119991 Russia*
** e-mail: ulianan@rambler.ru*

Received June 5, 2018; revised August 30, 2018; accepted September 28, 2018

Abstract—Interdiffusion and phase equilibrium in the system composed of polystyrene and statistical copolymers of butyl acrylate and styrene were studied by optical interferometry. The diagrams of the phase state were for the first time plotted and analyzed; pair interaction parameters were determined. The obtained diagrams are characterized by an upper critical solution temperature (UCST). The dependence of the interaction parameter on copolymer composition, polystyrene molecular weight, and temperature was shown. The data of interdiffusion of polystyrene into copolymers (and vice versa) are presented; they vary within 10^{-7}–10^{-11} cm^2/s. The activation energy of diffusion was calculated. No influence of structural heterogeneity of macromolecules of statistical copolymers on phase characteristics, translational diffusion coefficients, and coordinate of the diffusion front was registered.

DOI: 10.1134/S0965545X19020020

The main problem of analysis and prediction of processes of inter- and self-diffusion in binary and multicomponent polymer systems is related to the lack of quantitative data on the contribution of the architecture given by synthesis of a macromolecular compound to the numerical values of partial diffusion coefficients of macromolecules. It can be stated that at present the problem of the effect of molecular weight and molecular weight distribution on translational mobility of macromolecules [1–5] is solved owing to emergence of research dedicated to the influence of the nature of end groups [6]. However, the data on translational mobility of macromolecules in composition heterogeneous, branched, star, alternating block, and graft copolymers are at the initial stage of development [7].

The data on diffusion and phase properties of copolymer–homopolymer systems should be taken into account to solve these problems. Controlled synthesis of copolymers with set architecture of macromolecular chains under conditions of "living" anionic polymerization and radical polymerization with reversible deactivation of chain has been actively developed in polymer chemistry in recent decades. This technique allows obtaining composition homogeneous statistical and gradient copolymers and star, alternating, and block copolymers [8–18].

Previously [19], we studied phase equilibrium and interdiffusion of the polystyrene–poly(*n*-butyl acrylate) (PBA) system within a wide range of molecular weights of components. The majority of these systems are characterized by diagrams exhibiting amorphous layering and UCST. Pair interaction parameters were

Table 1. Characteristics of experimental objects

Object	Styrene content in copolymer, mol %	$M_n \times 10^{-3}$	$Đ$	T_g, K
PBA	0	35.0	1.17	223
PS-1	100	0.74	1.11	303
PS-2	100	1.14	1.07	343
PS-3	100	2.33	1.07	348
PS-4	100	4.1	1.00	353
PS-5	100	9.0	1.01	373
PS-6	100	30.0	1.02	373
stat-CBAS-8*	8	54.0	1.58	238
stat-CBAS-21*	21	48.0	1.53	252
stat-CBAS-35*	35	50.0	1.56	275
stat-CBAS-17	17	47.0	1.40	248
stat-CBAS-25	25	50.0	1.47	260

determined in terms of the classical Flory–Huggins theory; their dependence on the molecular weight of PS and temperature was registered. The possibility to predict generalized phase state diagrams of the PS–PBA system (molecular weight up to 10^6) was shown.

The started study of solubility and interdiffusion in binary systems containing copolymers (*n*-butyl acrylate–*co*-styrene) of different composition (including statistical, gradient, and, in particular, composition homogeneous and narrow-dispersed ones) as one of the components and PS and PBA homopolymer macromolecular probes as the second component is the natural sequel of these investigations. The results of these investigations were generalized in the present work.

EXPERIMENTAL

PBA, PS, and their statistical copolymers of various microstructure obtained by classical radical copolymerization (*stat*-CBAS*) and reversible chain transfer copolymerization (*stat*-CBAS) were used as experimental objects. The styrene content in copolymers was varied within 10–40 mol % (Table 1). The conditions of synthesis and the method of determination of the composition of copolymers were described in [20].

The solubility of polymers was studied by laser microinterferometry [21, 22]. Films of PS and copolymers 120–150 μm thick were used for all measurements by the pressing method. The experimental technique was similar to the traditional one. Film samples (5 × 10 mm) were placed between two optically transparent glasses 5 mm thick; a semitransparent layer of metal (nichrome) characterized by a high refractive index was preliminarily applied to inner surface of the glasses. A small tilt angle (~5°) was formed using metal clamps of different thickness (for example, 100 and 120 μm for PS film 120 μm thick). The optical contact between the samples and the inner surface of the glasses was established at a temperature 20–30 K higher than the glass transition temperature. Micrometric screws were used to set the largest dimension of sample perpendicularly to the tilt rib. In this case, the direction of diffusion flow coincides with the direction of interference fringes. The obtained cell was placed into a thermostatted diffusion cuvette; the accuracy of temperature maintenance in the cuvette was ±1 K. Then a capillary was filled with melts of PBA or *stat*-CBAS characterized by rather high fluidity (see Table 1). The moment of phase contact was considered the start of the interdiffusion process.

A He–Ne laser (wavelength of 632 nm) was used as a light source. The interference pattern was registered

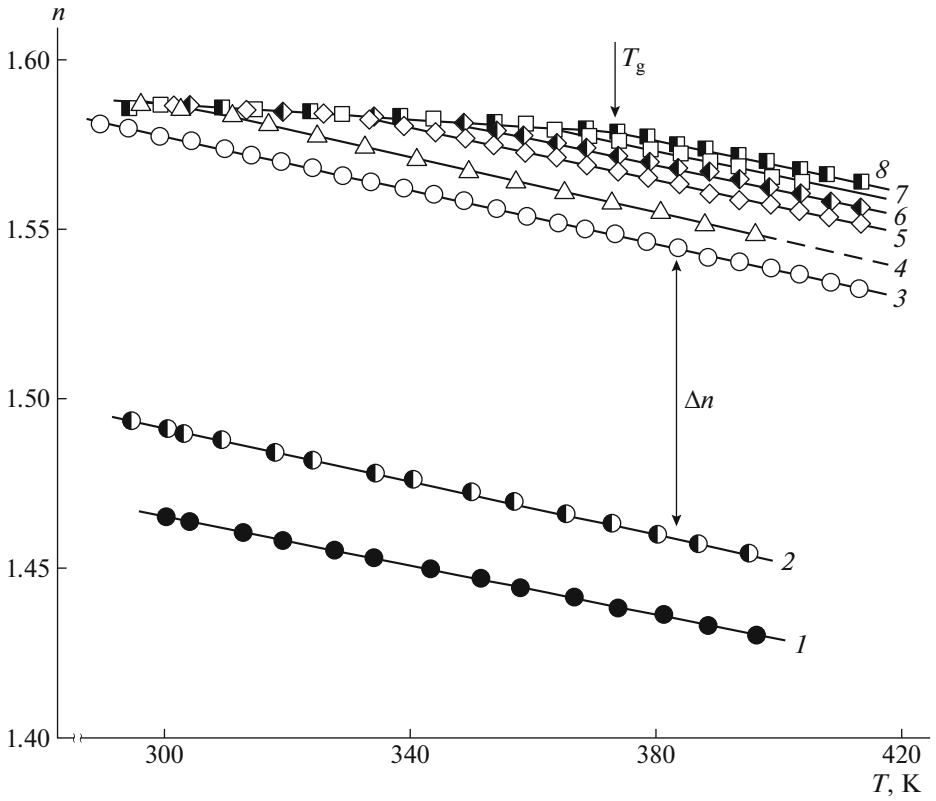

Fig. 1. Temperature dependence of refractive index for PBA (*1*), *stat*-CBAS-17 (*2*), PS-1 (*3*), PS-2 (*4*), PS-3 (*5*), PS-4 (*6*), PS-5 (*7*), and PS-6 (*8*).

using digital video camera; the image was sent to a PC. Measurements were performed under stepwise increase/decrease in temperature within 280–500 K. The processing of the interference pattern was the same as the traditional one.

Preliminary experiments allowed obtaining data on the temperature dependence of the refractive index of PS, PBA, and copolymers to estimate the quantity of interference fringes within the interdiffusion region for every polymer–copolymer pair (Fig. 1).

Thus, for PS-4, the difference between the refractive indices of PS and PBA is 0.13 at temperatures higher than T_c (for example, 380 K); for PS and *stat*-CBAS-17, it is 0.11, which corresponds to the formation of up to 40–45 interference fringes within the interdiffusion region. This means that the increment of composition (concentration) is registered with accuracy of 2.4 vol % in transition from one of interference fringe to another. These data was used for the determination of compositions of coexisting phases in systems characterized by amorphous layering.

RESULTS AND DISCUSSION

Interdiffusion Regions

Typical interference patterns of regions of phase conjugation of PBA and copolymers obtained by the classical radical copolymerization *stat*-CBAS* are given in Figs. 2a and 2b. The information concerning the interaction between PS and PBA homopolymers is given for comparative purposes in Fig. 2c [19]. It is seen that the PS–PBA interdiffusion region is a superposition of five regions: pure homopolymers, interfacial boundary (dark line in the middle of concentration profile), and regions of partial dissolution of PBA in PS (and vice versa; regions to the left and to the right of the interfacial boundary, respectively). In the case of interaction between copolymers and PBA, complete mutual solubility of components is observed at the same temperature. The concentration profile characterizing the composition distribution within the interdiffusion region is identified for these systems at all concentrations from PBA to *stat*-CBAS.

The influence of PS molecular weight on interdiffusion of components was illustrated in Figs. 3 and 4 by example of copolymers *stat*-CBAS* and *stat*-CBAS synthesized by classical polymerization and reversible chain transfer polymerization. It is seen that complete dissolution of components in each other is observed in the case of PS characterized by $M \le 1.2 \times 10^3$ (Fig. 3).

The solubility of homopolymer in copolymer decreases as the molecular weight of homopolymer grows. For PS-4 ($M_n = 4.1 \times 10^3$), the interfacial boundary separating the regions of copolymer dissolution in PS

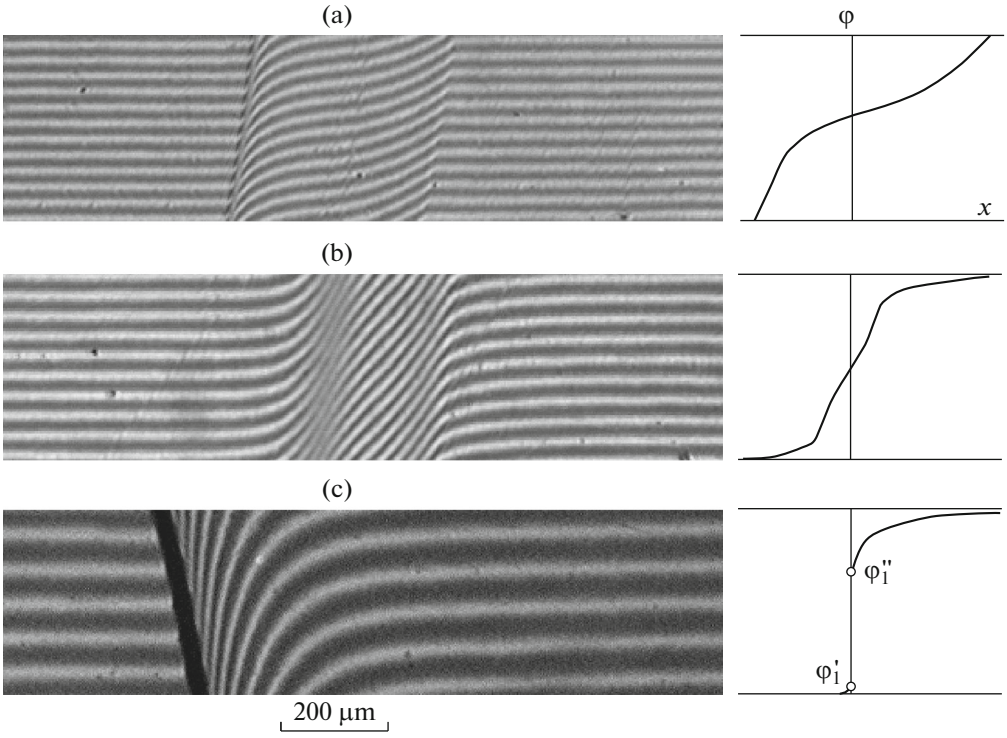

Fig. 2. Interference patterns of interaction of copolymers *stat*-CBAS-8* (a) and *stat*-CBAS-21* (b) with PBA and corresponding profile lines of concentration distribution at 333 and 413 K, respectively; (c) interference pattern of interdiffusion in PS-4–PBA system at 413 K; φ_1' and φ_1'' are the compositions of coexisting phases.

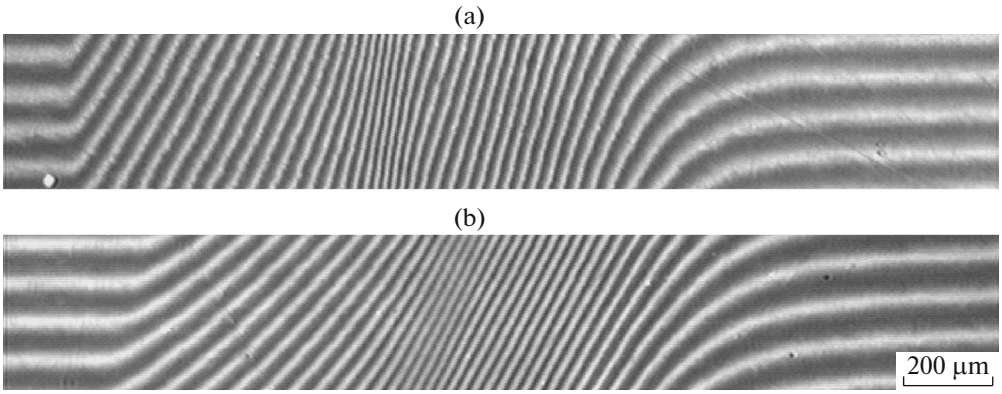

Fig. 3. Interference patterns of interaction of PS-2 with *stat*-CBAS-8* (a) and *stat*-CBAS-21* (b) copolymers at 413 K.

(to the left of the interfacial boundary) and PS dissolution in copolymer (to the right of the boundary) is formed within the region of diluted solutions of copolymer in PS. For PS-5 ($M_n = 9.0 \times 10^3$), the region of copolymer dissolution in homopolymer is degenerated. Such systems are considered systems with one-way diffusion [23, 24]. The components are almost incompatible for PS characterized by $M_n > 30.0 \times 10^3$ (Fig. 4c). In this case, the interference patterns are composed of superposition of three zones: two regions of pure components and interfacial boundary region.

The concentrations of saturated solutions φ' and φ'' corresponding to the compositions of coexisting phases, i.e., solubility of copolymers in PS (and vice versa) at the given temperature, are estimated under isothermal conditions in the neighborhood of the interfacial boundary (φ' and φ'' are the volume fractions of homopolymer in gradient solution) [25]. Such structure of the transition concentration gradient region of phase conjugation is observed for all studied PS–*stat*-CBAS pairs irrespective of the synthesis conditions of copolymers.

Additional data on the mechanism of mixing of components was obtained according to the kinetics of motion of diffusion fronts of homopolymers (Fig. 5) into the copolymer phase (curves *1'–5'*). It is seen that the shift of coordinates of fronts is linear in $X–t^{1/2}$ coordinates, indicating the diffusion mechanism of spontaneous mixing of homopolymers with copolymers. The slope of $X–t^{1/2}$ straight lines decreases as the PS molecular weight is raised, indicating the decrease in mass transfer rate. It should be mentioned that the coordinates of the Boltzmann–Matano plane remain constant within the whole observation of interdiffusion, which demonstrates the absence of volume contraction at mixing of polymers. Thus, one can conclude that a traditional diffusion mechanism of mixing of polymers and copolymers is observed in the PS–*stat*-CBAS and PS–*stat*-CBAS* systems. The specific features of one system or another are pronounced in the length of the interdiffusion region and numerical values of diffusion coefficients and compositions of coexisting phases.

Phase Diagrams

Phase diagrams of PS blends with copolymers (Figs. 6, 7) were plotted using the temperature dependences of composition of coexisting phases. It is seen that mutual solubility of the components of the mixtures increases as the temperature is raised; i.e., the systems are characterized by UCST. However, it was impossible to experimentally determine UCST because the position of critical values of temperature is located in the region corresponding to the thermolysis of the trithiocarbonate group and formation of polymer characterized by lower molecular weight [26, 27]. Theoretical estimates of the position of the binodal dome were performed in terms of the approach introduced and previously approved in [19] (dotted lines in Figs. 6, 7).

The increase in molecular weight of PS shifts the binodal curves of all systems toward the region of diluted solutions of PS. In this case, the character of the phase structure in the heterogeneous region of diagram, which can be classified as "matrix–inclusion" structural type, remains constant (SEM image in Fig. 6).

The solubility of PS in the copolymer phase (and vice versa) increases as the content of styrene units increases in both *stat*-CBAS and *stat*-CBAS* at transition from PBA to copolymers. This effect is most pronounced at plotting the isothermal cross section of the phase diagram (Fig. 8). Let us recall that in this case the binodal dome corresponding to the content of styrene in copolymers is about 50–55%; at this content, complete compatibility of components is observed. The critical composition of the system is determined by the ratio of molecular weights; it lies within 0.6–0.7 volume fractions of PS.

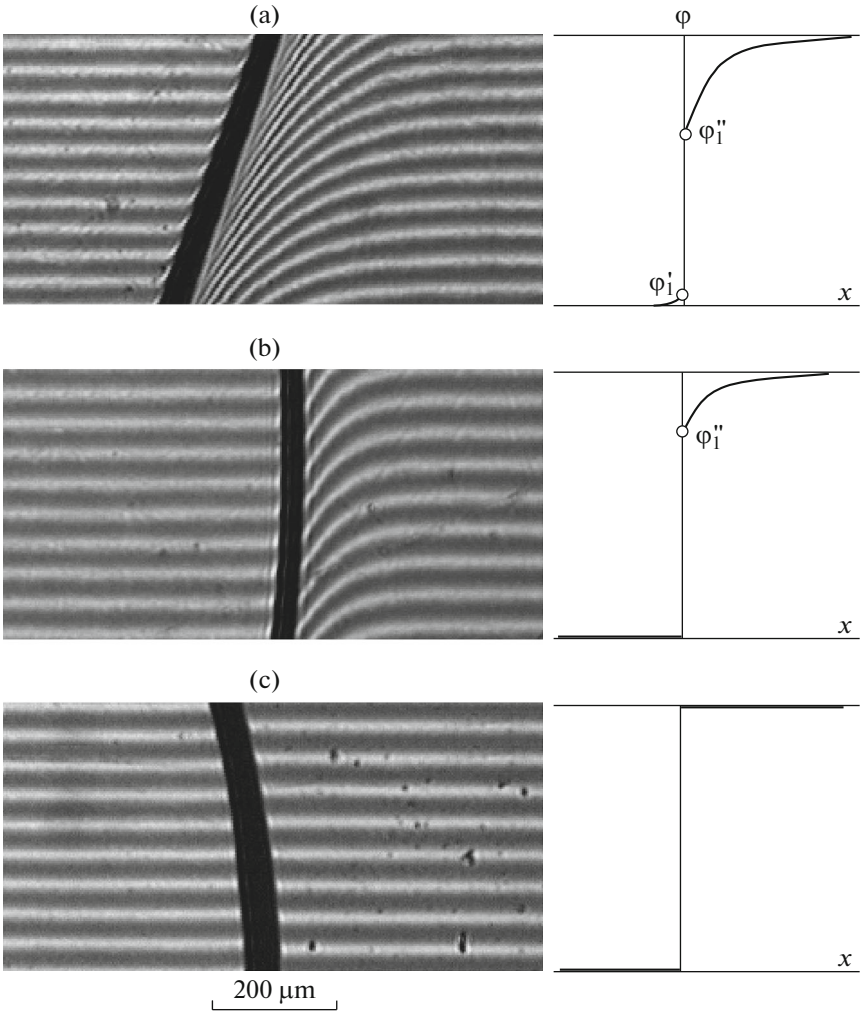

Fig. 4. Interference patterns of interaction of *stat*-CBAS-17 copolymer with PS-4 (a), PS-5 (b), and PS-6 (c) at 413 K and corresponding profile lines of concentration distribution.

The position of binodal fragments of the PS-5–*stat*-CBAS-8* and PS–*stat*-CBAS-17 systems shows that PS solubility is somewhat higher in the first case (Fig. 6, curves *2* and *3*). PS solubility in the copolymer obtained by the reversible chain transfer (curve *4*) is similar to PS solubility in PBA (curve *1*). However, in our opinion, this result should not be related to the structural heterogeneity of macromolecules because *stat*-CBAS and *stat*-CBAS* copolymers differ in composition of macromolecules, the influence of which on solubility of components is higher than that of the structural factor. The mutual position of figurative points of copolymers on the boundary curve of the isothermal cross section of the phase diagram is evidence of this fact.

Thermodynamics of Mixing Process

It is well known that the equality of chemical potentials of every component in phases is the condition of thermodynamic equilibrium of two phases in binary systems. The condition of coexistence of two phases corresponding to two points on the binodal is the following:

$$\Delta\mu_1' = \Delta\mu_1'' \quad \text{and} \quad \Delta\mu_2' = \Delta\mu_2'',$$

where $\Delta\mu_i$ is the change in chemical potential of component in the first $\Delta\mu_i'$ and the second $\Delta\mu_i''$ phases.

Specific equations for chemical potentials of components are derived from the Flory–Huggins–Scott theory of polymer solutions [25] which introduces the following formula for the Gibbs free energy at mixing of two polymers in the mutual volume V:

$$\Delta G_{\text{mix}} = \frac{RTV}{V_r}\left[\frac{\varphi_1}{r_1}\ln\varphi_1 + \frac{\varphi_2}{r_2}\ln\varphi_2 + \chi_{12}\varphi_1\varphi_2\right], \quad (1)$$

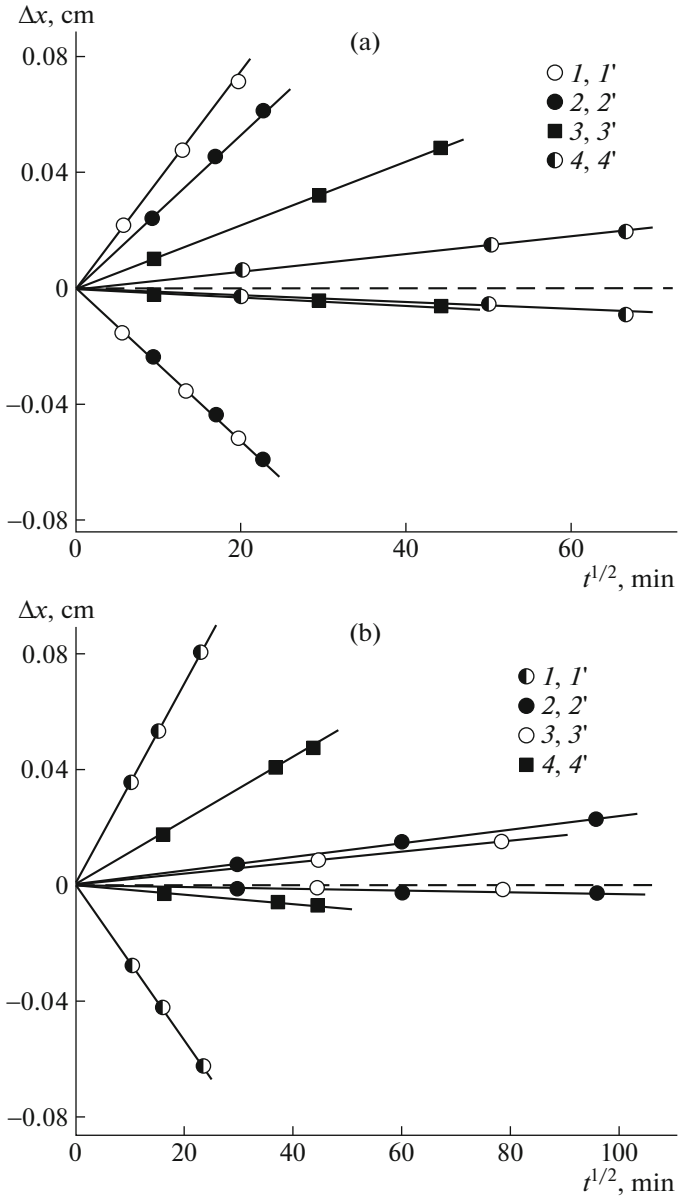

Fig. 5. Kinetics of motion of diffusion fronts at 393 K in (a) systems composed of *stat*-CBAS-8* copolymer with PS-2 (*1*, *1'*), PS-3 (*2*, *2'*), PS-4 (*4*, *4'*), and PBA–PS-3 (*3*, *3'*) and (b) systems composed of *stat*-CBAS-21* copolymer with PS-2 (*1*, *1'*), PS-4 (*2*, *2'*), PS-5 (*3*, *3'*), and PBA–PS-3 (*4*, *4'*); (*1*–*4*) kinetics of diffusion into phase of copolymer and PBA; (*1'*–*4'*) kinetics of diffusion into PS phase.

where V_r is the comparative volume, which is set to 100 cm^3/mol according to [28]; r are the degrees of polymerization of homopolymer and copolymer expressed in units of comparative volume (the values of weight average molecular weight were used for the calculation for copolymers); φ_1 and φ_2 are the volume fractions of homopolymer and copolymer, respectively; and χ is the pair interaction parameter characterizing the interaction between components. The following equations can be written for chemical potentials taking into account the concentration dependence of pair interaction parameter $\chi(\varphi_i)$:

$$\ln\varphi_1' + \left(1 - \frac{r_1}{r_2}\right)\varphi_2' + r_1\chi_{12}(\varphi_2')^2 = \ln\varphi_1'' + \left(1 - \frac{r_1}{r_2}\right)\varphi_2'' + r_1\chi_{12}(\varphi_2'')^2, \quad (2)$$

$$\ln\varphi_2' + \left(1 - \frac{r_2}{r_1}\right)\varphi_1' + r_2\chi_{21}(\varphi_1')^2 = \ln\varphi_2'' + \left(1 - \frac{r_2}{r_1}\right)\varphi_1'' + r_2\chi_{21}(\varphi_1'')^2, \quad (3)$$

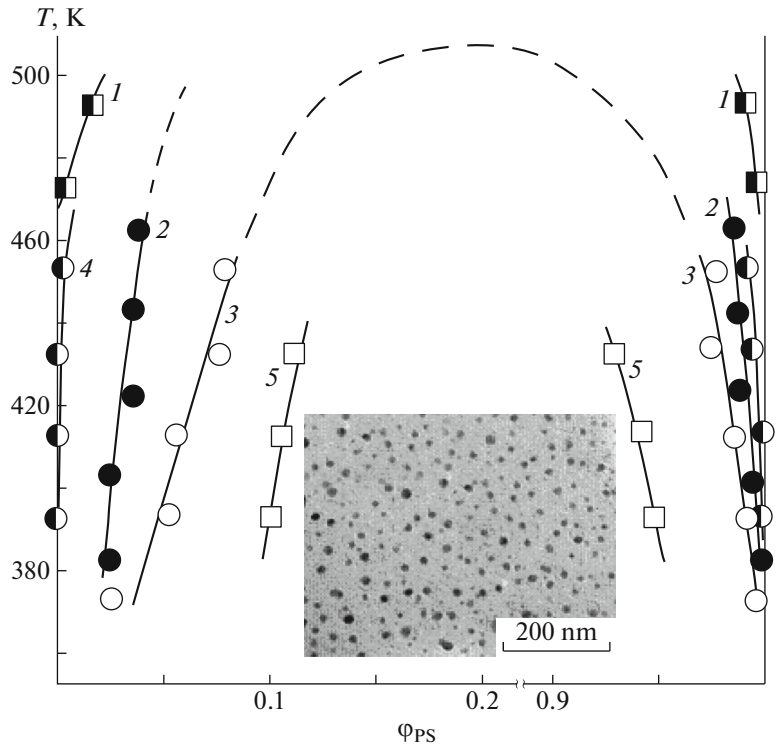

Fig. 6. Phase diagrams of systems PS-6–PBA (*1*), PS-5–*stat*-CBAS-8* (*2*), PS-5–*stat*-CBAS-17 (*3*), PS-6–*stat*-CBAS-17 (*4*), PS-5–*stat*-CBAS-25 (*5*), and PS-5–*stat*-CBAS-35* (SEM image of composition blend is given); here and in Fig. 7, dotted lines show the model diagram domes.

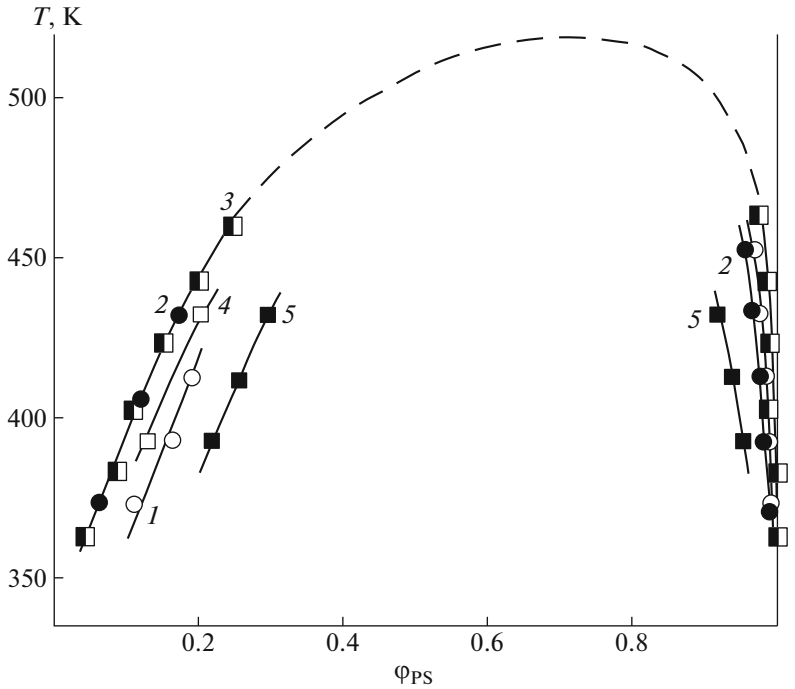

Fig. 7. Phase diagrams of systems PS-4–*stat*-CBAS-17 (*1*), PS-4–*stat*-CBAS-21* (*2*), PS-4–PBA (*3*), PS-4–*stat*-CBAS-25 (*4*), and PS-4–*stat*-CBAS-35* (*5*).

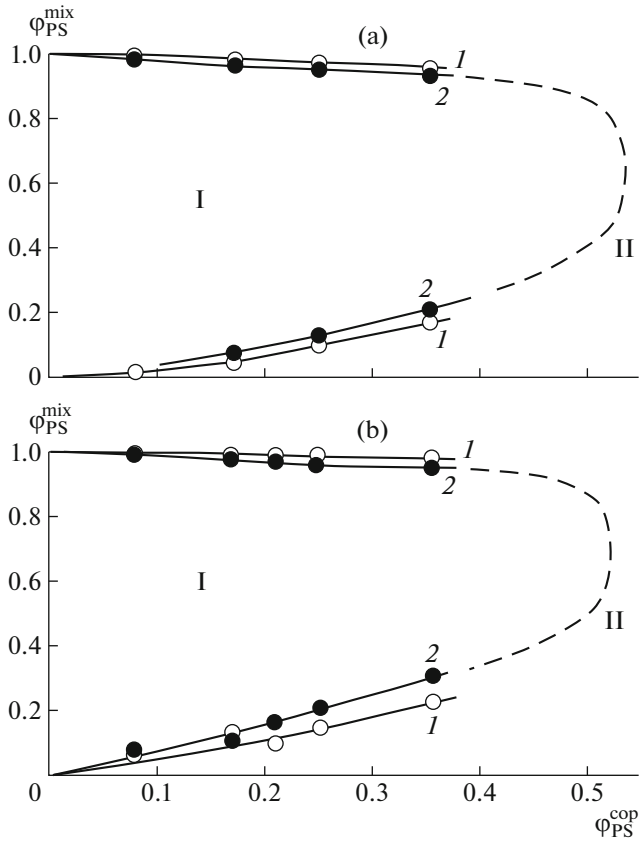

Fig. 8. Isothermal cross section of phase diagram at 393 (*1*) and 433 K (*2*) of systems PS-5 (a) and PS-4 (b); (I) heterogeneous state region; (II) true solution region.

where φ_i' is the volume fraction of the *i*th component in the first phase, φ_i'' is the volume fraction of the *i*th component in the second phase, $\chi_{12} = \chi + \frac{\partial \chi}{\partial \varphi_1}$, and $\chi_{21} = \chi + \frac{\partial \chi}{\partial \varphi_2}$.

The solution of Eqs. (1) and (2) with regard to the values χ_{12} and χ_{21} allows obtaining unambiguous calculation ratios which can be applied for binary polymer systems without taking into account the composition heterogeneity of macromolecules:

$$\chi_{12} = \frac{\ln\varphi_1'' - \ln\varphi_1'}{r_1((\varphi_2')^2 - (\varphi_2'')^2)} - \left(\frac{1}{r_1} - \frac{1}{r_2}\right)\frac{1}{\varphi_2' + \varphi_2''}, \quad (4)$$

$$\chi_{21} = \frac{\ln\varphi_2'' - \ln\varphi_2'}{r_1((\varphi_1')^2 - (\varphi_1'')^2)} - \left(\frac{1}{r_1} - \frac{1}{r_2}\right)\frac{1}{\varphi_1' + \varphi_1''}. \quad (5)$$

The numerical values of χ_{12} and χ_{21} were for the first time calculated using the composition of coexisting phases of these systems. It should be mentioned that the values of χ_{12} and χ_{21} almost coincide with each other (for example, for PS-4–*stat*-CBAS-17, $\chi_{12} = 0.036 \pm 0.003$, $\chi_{21} = 0.033 \pm 0.002$), which indicates the absence of concentration dependence of pair interaction parameters in the system.

The temperature dependences of χ_{12} are given in Fig. 9. It is seen that the values of the pair interaction parameter of PS–PBA and PS–*stat*-CBAS vary within a comparatively narrow range from 0.01 to 0.07; they are close to the critical value of pair parameter $\chi_{cr} = \frac{1}{2}\left(\frac{1}{\sqrt{r_1}} + \frac{1}{\sqrt{r_2}}\right)^2$. In this case, the current values $\chi_{12} > (\chi_{12})_{cr}$; this inequality indicates incompatibility (or partial compatibility) of PS–*stat*-CBAS blends.

Linear temperature dependences $\chi_{12}-1/T$ are observed for all studied systems; their slope which characterizes the enthalpy contribution to the energy of polymer interaction is positive, which is typical of systems with UCST. It should be mentioned that the UCST position can be estimated according to the point of intersection of extrapolated $\chi_{12}-1/T$ dependence to $(\chi_{12})_{cr}$.

The dependences of pair interaction parameters on copolymer composition of copolymers of butyl acrylate and styrene are generalized in Fig. 10. It is seen that the pair interaction parameter decreases as the content of styrene units in copolymer chain is raised; it asymptotically approaches the ultimate values which coincide with $(\chi_{12})_{cr}$. This dependence can be used for the estimation of the composition of copolymers (point of intersection of curves $\chi_{12} \cong (\chi_{12})_{cr}$) which corresponds to the region of compatibility of their mixtures with homopolymers. The critical value of φ_{PS} determined using the point of intersection of the curves $\chi_{12}(\varphi)$ and $(\chi_{12})_{cr}$ is 0.6–0.7 volume fractions of PS. This calculated value is in good accordance with the experimental data (see Fig. 8).

Diffusion Characteristics

It is known that two limiting composition regions $\varphi_1 \to 0$ and $\varphi_1 \to 1$ are the most interesting ones in binary systems; these regions correspond to the position of diffusion fronts in the copolymer and homopolymer phases. Here φ_1 is the concentration of

Table 2. Activation energy of diffusion in PS–acrylate copolymers systems

Diffusant	Diffusion medium	E_a, kJ/mol
PS-4	PBA	29.7
PS-4	*stat*-CBAS-8*	32.2
PS-4	*stat*-CBAS-17	32.6
PBA	PS-4	44.2
stat-CBAS-8*	PS-4	48.0
stat-CBAS-17	PS-4	48.5

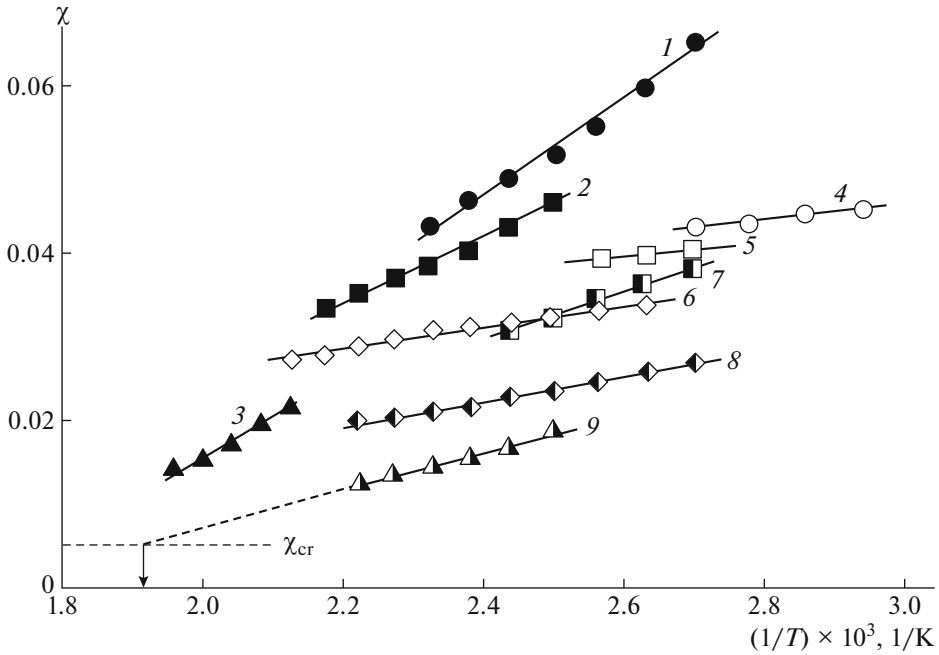

Fig. 9. Temperature dependence of pair interaction parameter PBA with PS-3 (*1*), PS-4 (*2*), and PS-6 (*3*); *stat*-CBAS-8* with PS-3 (*4*) and PS-5 (*5*); *stat*-CBAS-21* with PS-4 (*6*); and *stat*-CBAS-17 with PS-4 (*7*), PS-5 (*8*), and PS-6 (*9*).

PS in its solutions in copolymers. Precisely these data were used for the analysis of interdiffusion of copolymers and PS.

Figure 11 demonstrates the dependences of the coefficients of PS diffusion into copolymers (and vice versa) on copolymer composition. Obviously, in the first case ($\varphi_1 \to 0$), partial translation mobility of homopolymer molecules in the medium of styrene and butyl acrylate copolymer can be discussed; in the second case ($\varphi_1 \to 1$), translational mobility of copolymers in PS matrix is observed [29, 30]. In terms of a reptation model, such changes in the nature of the diffusion medium and diffusant mean that, in the first case, data on the influence of macromolecules of copolymer forming "tube walls" on the translational mobility of PS macromolecules are predominantly obtained. In the second case, data on the influence of the structure of copolymer macromolecules moving "along the tube" formed by PS macromolecules on the diffusion coefficient is obtained [29, 30].

It is interesting to mention that the coefficients of diffusion of PS macromolecules into copolymers (D_{12}) are higher than the coefficients of diffusion of copolymer macromolecules into PS (D_{21}). Such ratio between diffusion coefficients D_{12} and D_{21} is preserved at all values of temperature and is related to the difference between the molecular weights of PS and copolymers. The closeness of positions of figurative points of *stat*-CBAS and *stat*-CBAS* copolymers on concentration dependences of partial diffusion coefficients D_{12} and D_{21} means that the possible differences in composition heterogeneity of copolymers obtained by different synthesis techniques within the region of the true solutions of the phase diagrams exhibit a fluctuating character and do not affect the translation diffusion coefficients and coordinate of the diffusion front.

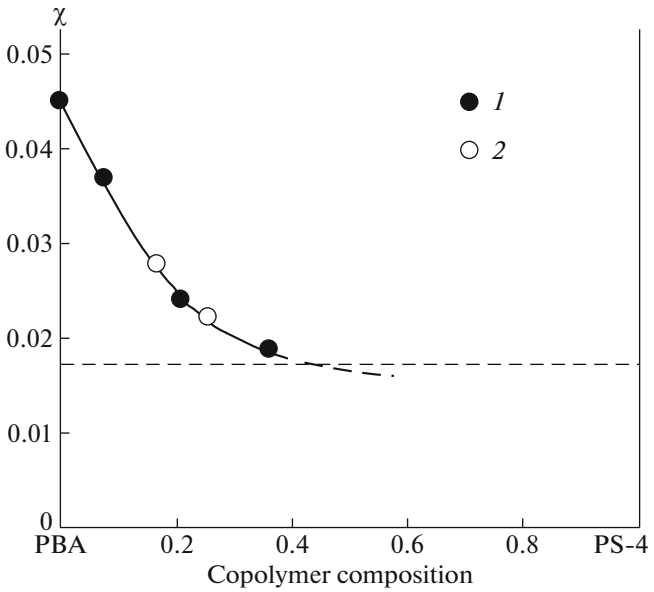

Fig. 10. Dependence of pair interaction parameter on copolymer composition at 400 K in systems containing PS-4: (*1*) PBA (*y* axis) and *stat*-CBAS*; (*2*) *stat*-CBAS.

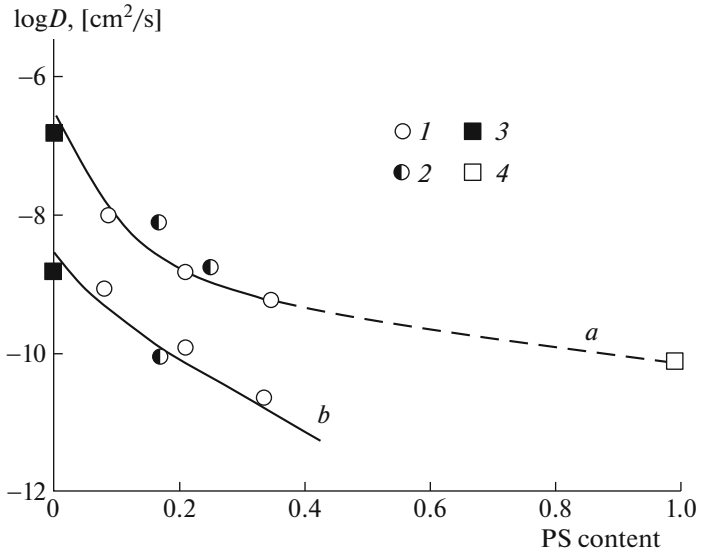

Fig. 11. Dependence of diffusion coefficient on copolymer composition at 393 K in copolymer phase at diffusion of PS-4 into matrix of PBA or copolymers (*a*) and in PS phase at PBA or copolymer diffusion into PS-4 matrix (*b*): (*1*) *stat*-CBAS*; (*2*) *stat*-CBAS; (*3*) PBA; (*4*) PS.

The results concerning the activation energy of diffusion allow drawing the same conclusion (Table 2).

Thus, a complex study of diffusion processes and solubility of PS characterized by different molecular weights in statistical copolymers of *n*-butyl acrylate and styrene of varying composition was performed. It was shown that the synthesis technique which affects the molecular weight and composition dispersion of copolymers, i.e., structural heterogeneity of macromolecules of statistical copolymers, exhibits less influence on the phase and diffusion parameters than the differences in composition of copolymers.

ACKNOWLEDGMENTS

This work was supported by the Russian Foundation for Basic Research (project no. 17-03-00197A) and by the RF Government task (no. AAAA-A18-118030690046-0).

REFERENCES

1. A. A. Shcherbina, M. V. Vokal', and A. E. Chalykh, Russ. Chem. Bull. **64**, 791 (2015).
2. P. F. Green and J. Ch. Barbour, J. Non-Cryst. Solids **235**, 640 (1998).
3. K. Tsubaki and K. Ishizu, Polymer **42**, 8387 (2001).
4. A. I. Maklakov, V. D. Skirda, and N. F. Fatkullin, *Self-Diffusion in Solutions and Melt of Polymers* (Kazan State Univ., Kazan, 1987) [in Russian].
5. A. E. Chalykh and V. B. Zlobin, Russ. Chem. Rev. **57**, 504 (1998).
6. A. A. Poteryaev, Candidate's Dissertation in Chemistry (Inst. Fiz. Khim. Elektrokhim. RAN, Moscow, 2018).
7. *Diffusion in Polymers (Plastics Engineering),* Ed. by P. Neogi (CRC Press; New York; Basel; Hong Kong, 1996).
8. L. Wu, E. W. Cochran, T. P. Lodge, and F. S. Bates, Macromolecules **37**, 3360 (2004).
9. R. J. Spontak and S. D. Smith, J. Polym. Sci., Polym. Phys. Ed. **39**, 947 (2001).
10. E. A. Eastwood and M. D. A. Dadmun, Macromolecules **34**, 740 (2001).
11. Y. Zhou, K. Jiang, Q. Song, and S. Liu, Langmuir **23**, 13076 (2007).
12. Z. Jia, X. Xu, Q. Fu, and J. Huang, J. Polym. Sci., Part A: Polym. Chem. **44**, 6071 (2006).
13. Z. Jia, C. Liu, and J. Huang, Polymer **47**, 7615 (2006).
14. D. Pavlovic, J. G. Linhardt, J. F. Kunzler, and D. A. Shipp, J. Polym. Sci., Part A: Polym. Chem. **46**, 7033 (2008).
15. Y. Nagata, J. Masuda, A. Noro, D. Cho, A. Takano, and Y. Matsushita, Macromolecules **38**, 10220 (2005).
16. J. Hong, Q. Wang, and Z. Fan, Macromol. Rapid. Commun. **27**, 57 (2006).
17. P. Lei, Q. Wang, J. Hong, and Y. Li, J. Polym. Sci., Part A: Polym. Chem. **44**, 6600 (2006).
18. Q. Wang, Y. X. Li, J. Hong, and Z. Q. Fan, Chin. J. Polym. Sci. **24**, 593 (2006).
19. A. E. Chalykh, U. V. Nikulova, and A. A. Shcherbina, Polym. Sci., Ser. A **57**, 445 (2015).
20. E. V. Chernikova, V. V. Yulusov, E. S. Garina, Yu. V. Kostina, G. N. Bondarenko, and A. Yu. Nikolaev, Polym. Sci., Ser. B **55**, 176 (2013).
21. A. Ya. Malkin and A. E. Chalykh, *Diffusion and Viscosity of Polymers: Measurement Techniques* (Khimiya, Moscow, 1979) [in Russian].

22. A. E. Chalykh, A. I. Zagaitov, V. V. Gromov, and D. P. Korotchenko, *Optical Diffusiometer "ODA-2": Manual* (Inst. Fiz. Khim. RAN, Moscow, 1996) [in Russian].
23. A. E. Chalykh, *Water Diffusion in Polymer Systems* (Khimiya, Moscow, 1987) [in Russian].
24. A. A. Tager, *Physics and Chemistry of Polymers: Tutorial for Chemical Facultiesof Universities,* Ed. by A. A. Askadskii (Nauchnyi mir, Moscow, 2007) [in Russian].
25. A. E. Chalykh, V. K. Gerasimov, and Yu. M. Mikhailov, *Phase State Diagrams of Polymer Systems* (Yanus-K, Moscow, 1998) [in Russian].
26. E. V. Chernikova, A. V. Plutalova, E. S. Garina, and D. V. Vishnevetsky, Polym. Chem. **7**, 3622 (2016).
27. U. V. Nikulova and A. E. Chalykh, in *Structure and Dynamics of Molecular Systems,* Ed. by A. A. Shcherbina (Inst. Fiz. Khim. Elektrokhim. RAN, Moscow, 2017), Issue 4, p. 177 [in Russian].
28. *Polymer Blends,* Ed. by. D. R. Paul and S. Newman (Acad. Press, New York; San Francisko; London, 1978), Vol. 1.
29. A. A. Shcherbina, Doctoral Dissertation in Chemistry (Inst. Fiz. Khim. Elektrokhim. RAN, Moscow, 2016).
30. P.-G. de Gennes, *Scaling Concepts in Polymer Physics* (Cornell Univ. Press, Ithaca; New York, 1979).

Translated by P. Vlasov